Two-stream instability with time-dependent drift velocity

Hong Qin[1,2] and Ronald C. Davidson[1]
[1]Plasma Physics Laboratory, Princeton University, Princeton, New Jersey 08543, USA
[2]Department of Modern Physics, University of Science and Technology of China, Hefei, Anhui 230026, China

(Received 1 May 2014; accepted 12 May 2014; published online 26 June 2014)

The classical two-stream instability driven by a constant relative drift velocity between two plasma components is extended to the case with time-dependent drift velocity. A solution method is developed to rigorously define and calculate the instability growth rate for linear perturbations relative to the time-dependent unperturbed two-stream motions. Stability diagrams for the oscillating two-stream instability are presented over a large region of parameter space. It is shown that the growth rate for the classical two-stream instability can be significantly reduced by adding an oscillatory component to the relative drift velocity. © *2014 AIP Publishing LLC*. [http://dx.doi.org/10.1063/1.4885076]

The electrostatic two-stream instability is a classical plasma physics problem that has been extensively studied. It is also of practical importance in many application areas. For example, it has been discovered that in high intensity proton accelerators, as the proton beam passes through the electron background resulting from residual gas ionization or secondary emission, the two-stream instability driven by the relative velocity between electrons and protons can significantly limit the intensity of the proton beams.[1–5] In astrophysics, the electron-positron two-stream instability of pair plasmas in a pulsar magnetosphere[6,7] has been identified as an important physical process, which has been experimentally simulated in the laboratory.[8,9] As a potential stabilization scheme, it has been suggested that a time-dependent relative drift velocity between the plasma components may reduce the growth rate of the instability.[4,10,11] This type of dynamical stabilization scheme for the two-stream instability has been experimentally studied.[10] In general, dynamic stabilization is a technique that can be applied to a variety of instabilities. Another example is the dynamic stabilization of the Rayleigh-Taylor instability for inertial confinement fusion experiments.[12–18] In Ref. 19, the concept of dynamic mitigation was developed for general types of instabilities. On the other hand, a purely oscillatory relative drift velocity may be unstable as well. This is the so-called oscillating two-stream instability,[20–23] which is an interesting problem in its own right. It has been studied for laboratory plasmas[24–26] as well as for ionospheric heating experiments.[27] In the literature, the oscillating two-stream instability has been treated mostly as a parametric instability process.

The question to address for the two-stream instability with time-dependent drift velocity is whether the time-dependent relative drift motion or oscillation between the two components of the plasma is stable. From a mathematical perspective, we are studying the stability of a time-dependent solution of the differential equations describing the collective dynamics of the plasma. Since the unperturbed solution under investigation is time-dependent, different temporal Fourier harmonics of the perturbation are coupled, and the stability properties of the system cannot be described by a simple dispersion relation as in the case of time-independent equilibrium solutions. Because of this challenging feature, most of the theoretical studies in the past have been based on asymptotic analyses for a special set of parameters, and a thorough understanding of the general properties of the instability has not been developed. For example, a stability diagram for the oscillating two-stream instability in general parameter space has not been charted.

In the present study, we have developed a method to calculate the linear stability properties of the two-stream dynamics for arbitrary system parameters and time-dependent relative velocity. For periodic oscillating relative velocity, the linear dynamics can be characterized by a one-period map from which the growth rate of the perturbation can be rigorously defined and calculated. Using this tool, we are able to obtain a comprehensive picture of the linear two-stream stability driven by a general time-dependent drift velocity. As a theoretical study, our analysis is based on a fluid model, and the time-dependent relative velocity is induced by a time-dependent applied electric field. For simplicity, the unperturbed solution is assumed to be spatially homogeneous.

For the purely oscillatory two-stream solution, the stability diagrams are presented over the entire parameter space. It is found that the growth rate and stability regions depend on the oscillation frequency ω_0 and the strength of the relative velocity V_d in a complex manner. However, over a large range of parameter space, there exist band structures in the stability diagram. For dynamic stabilization of the two-stream instability with a constant relative velocity achieved by adding an oscillatory relative velocity, it is found that dynamic stabilization does exist in certain parameter regimes. It is especially prominent for two-stream interactions with small mass-ratio, as in the case of a positron beam streaming through a background electron population. As the mass-ratio increases towards that of a hydrogen plasma, the stabilizing effect becomes less effective.

The paper is organized as follows. The fluid equations governing the electrostatic two-stream interaction with time-dependent relative velocity are first introduced, followed by a description of the analytical and numerical methods used to solve the system of equations. The main numerical results are then displayed with a discussion of the physics revealed by these numerical calculations.

We consider a two-component plasma whose 1D electrostatic dynamics in the z-direction is governed by the fluid-Poisson equations

$$\frac{\partial n_j}{\partial t}+\frac{\partial}{\partial z}(n_j v_j)=0, \tag{1}$$

$$\frac{\partial v_j}{\partial t}+v_j\frac{\partial v_j}{\partial z}+\frac{1}{n_j m_j}\frac{\partial p_j}{\partial z}=\frac{e_j}{m_j}E, \tag{2}$$

$$\frac{\partial E}{\partial z}=\sum_j 4\pi e_j n_j. \tag{3}$$

Here, $j=1$, 2 is the index labeling plasma species. Thermal effects are modeled by a simple adiabatic law with

$$p_j=\frac{p_{j0}}{\hat{n}_j^{\gamma_j}}n_j^{\gamma_j}, \tag{4}$$

where $p_{j0}=\hat{n}_j\hat{T}_j=const$, $\hat{n}_j=const$, $\hat{T}_j=const$ and γ_j is the poly-tropic index for the adiabatic dependence of p_j on n_j. The unperturbed dynamics is the time-dependent homogeneous solution specified by

$$n_j^0=\hat{n}_j, \tag{5}$$

$$v_j^0(t)=v_{j0}+\frac{e_j}{m_j}\int_0^t dt' E_0(t'). \tag{6}$$

The unperturbed velocity $v_j^0(t)$ is driven by the time-dependent externally applied electrical field $E_0(t)$. This setup has been experimentally demonstrated by Decker and Levin.[10] The unperturbed density is assumed to be constant with overall charge neutrality $\sum_j e_j n_j^0=0$.

We consider small perturbations $\tilde{\rho}_j=e_j\tilde{n}_j$, $\tilde{v}_j$ and $\tilde{E}$ relative to the time-dependent unperturbed solutions. The linearized fluid equations can be easily reduced to two coupled equations in terms of $\tilde{\rho}_j$

$$\left(\frac{\partial}{\partial t}+v_1^0\right)\left(\frac{\partial}{\partial t}+v_1^0\right)\tilde{\rho}_1-v_{T1}^2\frac{\partial^2}{\partial z^2}\tilde{\rho}_1=-\omega_{p1}^2(\tilde{\rho}_1+\tilde{\rho}_2), \tag{7}$$

$$\left(\frac{\partial}{\partial t}+v_2^0\right)\left(\frac{\partial}{\partial t}+v_2^0\right)\tilde{\rho}_2-v_{T2}^2\frac{\partial^2}{\partial z^2}\tilde{\rho}_2=-\omega_{p2}^2(\tilde{\rho}_1+\tilde{\rho}_2), \tag{8}$$

where $\omega_{pj}^2=4\pi\hat{n}_j e_j^2/m_j$ and $v_{Tj}^2=\gamma_j T_j/m_j$. Because $v_j^0(t)$ depends on time, but not on the spatial coordinate, we can Fourier-decompose the spatial dependence of $\tilde{\rho}_j$, and assume $\tilde{\rho}_j\sim\exp[ikz]$, where k is the wavenumber of the perturbation. Equations (7) and (8) then reduce to the coupled ordinary differential equations with time-dependent coefficients

$$\left(\frac{d}{dt}+kv_1^0\right)^2\tilde{\rho}_1+k^2v_{T1}^2\tilde{\rho}_1=-\omega_{p1}^2(\tilde{\rho}_1+\tilde{\rho}_2), \tag{9}$$

$$\left(\frac{d}{dt}+kv_2^0\right)^2\tilde{\rho}_2+k^2v_{T2}^2\tilde{\rho}_2=-\omega_{p2}^2(\tilde{\rho}_1+\tilde{\rho}_2). \tag{10}$$

When the drift velocity v_j^0 does not depend on time, corresponding to $E_0(t)=0$, we can assume $\tilde{\rho}_j\sim\exp[-i\omega t]$, and Eqs. (9) and (10) recover the expected dispersion relation

$$\frac{\omega_{p1}^2}{(\omega-kv_1^0)^2-k^2v_{T1}^2}+\frac{\omega_{p2}^2}{(\omega-kv_2^0)^2-k^2v_{T2}^2}=1. \tag{11}$$

For the general case of time-dependent v_j^0, the solutions of Eqs. (9) and (10) can be given by a time-dependent map from the initial conditions as

$$\begin{pmatrix}\tilde{\rho}_1\\ \tilde{\rho}_2\\ \dot{\tilde{\rho}}_1\\ \dot{\tilde{\rho}}_2\end{pmatrix}_t=M(t)\begin{pmatrix}\tilde{\rho}_1\\ \tilde{\rho}_2\\ \dot{\tilde{\rho}}_1\\ \dot{\tilde{\rho}}_2\end{pmatrix}_{t=0}.$$

Here, the map is specified by a time-dependent 4×4 matrix $M(t)$, which is independent of the initial conditions. It is completely determined by the unperturbed solutions and system parameters and can be easily calculated numerically by selecting four independent solutions of Eqs. (9) and (10). In particular, if $v_j^0(t)$ is a periodic function with periodicity T, then the solution is completely determined by the one-period map $M(T)$. The properties of long-time solutions are given by $M^n(T)$, $n\to\infty$. If $M(T)$ has an eigenvalue whose magnitude is larger than one, then the system is unstable. Otherwise, the system is stable. With these considerations, the appropriate definition of the growth rate of the dynamical system is[19]

$$\gamma\equiv\frac{\ln \mathrm{Max}[|\lambda_i|]}{T}, \tag{12}$$

where λ_i ($i=1$, 2, 3, and 4) are the eigenvalues of the one-period map $M(T)$.

We now present the numerical study of the stability properties of the two-stream interaction with time-dependent relative drift velocity. In the present study, we focus mainly on the effects of time-dependent drift velocity, and thus consider the most unstable case where thermal effects are neglected in Eqs. (9) and (10). It is convenient to normalize time by $1/\omega_{p1}$ and drift velocity by ω_{p1}/k. A straightforward analysis shows that the stability of the system depends on the drift velocity only through the relative velocity $v_d(t)\equiv v_1^0(t)-v_2^0(t)$ between the two components. Therefore, the dimensionless parameters for the system are the mass ratio m_2/m_1, charge ratio e_2/e_1, the normalized relative velocity $kv_d(t)/\omega_{p1}$, and the normalized ω_0/ω_{p1}.

The first case of our numerical study is the purely oscillating two-stream instability for $m_2/m_1=1$, such as occurs in the two-stream interactions between positrons and electrons[6,7] or between protons and anti-protons. The relative drift velocity is assumed be a periodic function with frequency $\omega_0=2\pi/T$ and amplitude $\hat{v}_d$, i.e.,

$$v_d(t)\equiv v_1^0(t)-v_2^0(t)=\hat{v}_d\sin(\omega_0 t).$$

Shown in Fig. 1 is the contour plot of the normalized growth rate γ/ω_{p1} as a function of ω_p/ω_0 and $k\hat{v}_d/\omega_{p1}$. The horizontal axis is chosen to be the inverse of the drive frequency normalized to the plasma frequency $\omega_p=\sqrt{\omega_{p1}^2+\omega_{p2}^2}=\sqrt{2}\,\omega_{p1}$, so that the figure has more resolution at frequencies smaller than the plasma frequency. The darkest region is

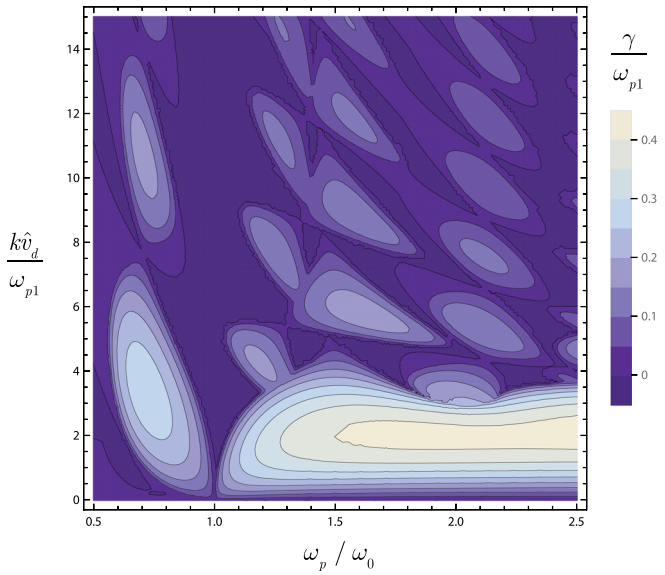

FIG. 1. Stability diagram for the oscillating two-stream instability. Contours of the normalized growth rate γ/ω_{p1} are plotted as functions of ω_p/ω_0 and $k\hat{v}_d/\omega_{p1}$ for $v_d(t) \equiv v_1^0(t) - v_2^0(t) = \hat{v}_d \sin(\omega_0 t)$, $e_2/e_1 = -1$, $m_2/m_1 = 1$, $\omega_{p2}/\omega_{p1} = 1$, and $\omega_p = \sqrt{\omega_{p1}^2 + \omega_{p2}^2}$. The darkest region is the region corresponding to stable oscillations.

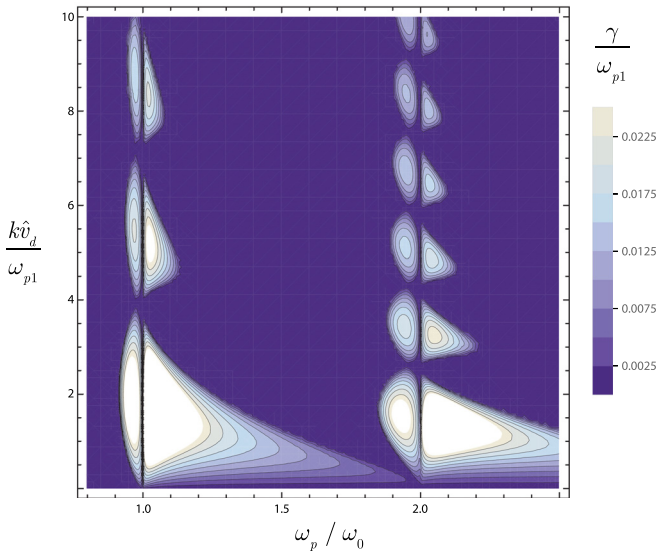

FIG. 2. Stability diagram of the oscillating two-stream instability. Contours of the normalized growth rate γ/ω_{p1} are plotted as functions of ω_p/ω_0 and $k\hat{v}_d/\omega_{p1}$ for $v_d(t) \equiv v_1^0(t) - v_2^0(t) = \hat{v}_d \sin(\omega_0 t)$ and $m_2/m_1 = 1836$. Here, $\omega_p = \sqrt{\omega_{p1}^2 + \omega_{p2}^2}$, and the darkest region is the region corresponding to stable oscillations. The stability/instability bands congregate at the subharmonics of the plasma frequency.

the region for stable oscillations, and the lighter regions are more unstable. It is evident that the growth rate depends on ω_p/ω_0 and $k\hat{v}_d/\omega_{p1}$ in a complex manner. However, over a wide range of parameter space, the stability/instability regions form a band structure. The vertical line $\omega_0 = \omega_p = \sqrt{2}\omega_{p1}$ is stable, which corresponds to stable plasma oscillations. However, there exist unstable regions nearby, especially when $k\hat{v}_d/\omega_{p1}$ is small. If the drive frequency is above or below the plasma frequency by a small amount, then the oscillations are unstable. This is a statement about the structural stability properties of plasma oscillations.

The band structure and proximity of unstable regions near the plasma frequency become more prominent as the mass-ratio increases, as displayed in Fig. 2, which is a similar contour plot of the growth rate for a hydrogen plasma with $m_2/m_1 = 1836$. The stability/instability bands become more structured, congregating at the subharmonics of the plasma frequency $\omega_p = \sqrt{\omega_{p1}^2 + \omega_{p2}^2} \approx \omega_{p1}$.

The next numerical study carried out is the dynamic stabilization of the two-stream instability with a component of oscillatory relative drift velocity. First, we look at the case where $m_2/m_1 = 1$ corresponding to positron and electron beams or proton and anti-proton beams. Figure 3 shows the normalized growth rate plotted as a function of $k\hat{v}_d/\omega_{p1}$ for three different time-dependent relative velocities. The first curve is for a DC drift velocity $v_d(t) = \hat{v}_d$, corresponding to the classical two-stream instability, whose growth rate γ/ω_{p1} can be solved for as a function of $k\hat{v}_d$ from the dispersion relation (11) with $v_{Tj} = 0$. The numerically calculated growth rate using the method according to Eq. (12) agrees exactly with that given by the dispersion relation (11). The second curve is for a purely oscillatory velocity of the form $v_d(t) = 1.6\,\hat{v}_d \sin(\omega_0 t)$ with $\omega_0 = 2.1\omega_{p1}$. For this set of parameters, the oscillating two-stream system is unstable. The third curve is for the combined velocity of the above two cases, i.e., $v_d(t) = \hat{v}_d[1 + 1.6\sin(2.1\omega_{p1}t)]$. We observe that even though the systems with the DC velocity or oscillatory velocity are unstable, the combination can reduce the maximum growth rate by about 75%. This effect can be explored for the purpose of designing possible stabilization schemes in practical applications. As the mass-ratio increases, this stabilization effect persists but becomes less prominent. This is demonstrated in Fig. 4, where $m_2/m_1 = 1836$. For this set of parameters, the reduction of the maximum growth rate is about 45%.

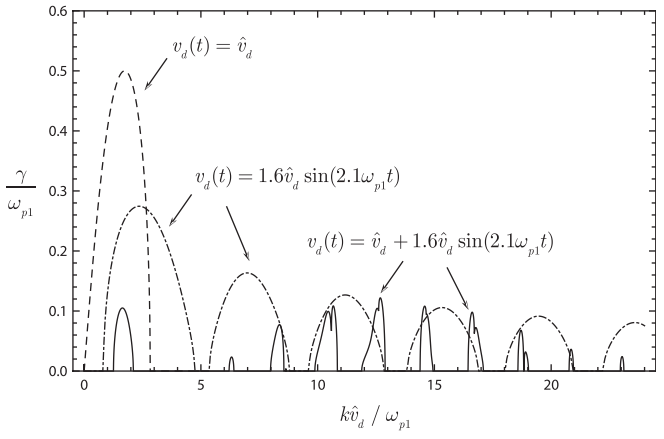

FIG. 3. Normalized growth rate γ/ω_{p1} plotted as a function of $k\hat{v}_d/\omega_{p1}$ for three choices of time-dependent velocity $v_d(t)$ for the case where $m_2/m_1 = 1$. The ratio between the amplitudes of the oscillatory and DC components of the drift velocity is 1.6.

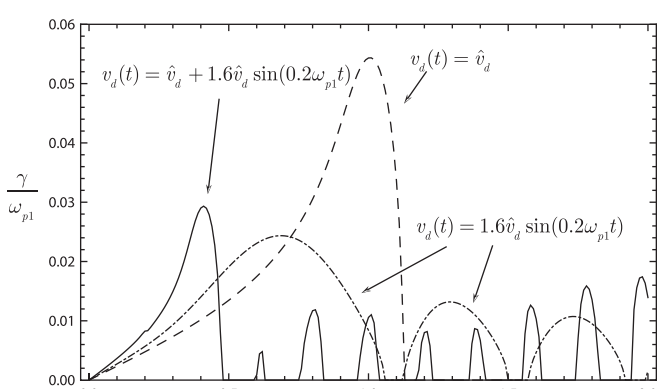

FIG. 4. Normalized growth rate γ/ω_{p1} plotted as a function of $k\hat{v}_d/\omega_{p1}$ for three choices of time-dependent velocity $v_d(t)$ for the case where $m_2/m_1 = 1836$. The ratio between the amplitudes of the oscillatory and DC components of the drift velocity is 1.6.

In conclusion, we have developed an effective theoretical method to investigate the two-stream instability with time-dependent drift velocity over a wide range of system parameters. The growth rate of the instability has been rigorously defined and calculated. The stability behavior of the system has a complex dependence on system parameters and exhibits a band structure over a large region of parameter space. The detailed information obtained regarding the dynamic stabilization of the two-stream instability can be used for the design of practical stabilization schemes. The fluid model in Eqs. (1)–(3) includes thermal effects. However, in this paper, we have chosen $v_{Tj} = 0$ and focused on the effects of time-dependent drift velocity in the numerical studies presented here. The influence of thermal effect as well as other physical factors, such as spatial inhomogeneities, is currently being investigated and will be reported in future publications.

This research was supported the U.S. Department of Energy (DE-AC02-09CH11466). We thank Joshua W. Burby for fruitful discussions.

[1]R. C. Davidson, H. Qin, P. H. Stoltz, and T. S. Wang, Phys. Rev. Spec. Top. - Accel. Beams **2**, 054401 (1999).
[2]H. Qin, R. C. Davidson, and W. W. Lee, Phys. Rev. Spec. Top. - Accel. Beams **3**, 084401 (2000).
[3]T.-S. F. Wang, P. J. Channell, R. J. Macek, and R. C. Davidson, Phys. Rev. Spec. Top.- Accel. Beams **6**, 014204 (2003).
[4]E. A. Startsev and R. C. Davidson, Nucl. Instrum. Methods Phys. Res., Sect. A **577**, 79 (2007).
[5]F. Zimmermann, Phys. Rev. Spec. Top. - Accel. Beams **7**, 124801 (2004).
[6]V. V. Usov, Astrophys. J. **320**, 333 (1987).
[7]E. Asseo, Plasma Phys. Controlled Fusion **45**, 853 (2003).
[8]R. G. Greaves and C. M. Surko, Phys. Rev. Lett. **75**, 3846 (1995).
[9]S. J. Gilbert, D. H. E. Dubin, R. G. Greaves, and C. M. Surko, Phys. Plasmas **8**, 4982 (2001).
[10]J. F. Decker and A. M. Levine, AIP Conf. Proc. **1**, 260 (1970).
[11]R. M. Chervin and A. K. Sen, Plasma Phys. **15**, 387 (1973).
[12]G. Wolf, Phys. Rev. Lett. **24**, 444 (1970).
[13]F. Troyon, Phys. Fluids **14**, 2069 (1971).
[14]S. Kawata, T. Sato, T. Teramoto, E. Bandoh, Y. Masubichi, and I. Takahashi, Laser Part. Beams **11**, 757 (1993).
[15]R. Betti, R. L. McCrory, and C. P. Verdon, Phys. Rev. Lett. **71**, 3131 (1993).
[16]S. Kawata, Y. Iizuka, Y. Kodera, A. I. Ogoyski, and T. Kikuchi, Nucl. Instrum. Methods Phys. Res., Sect. A **606**, 152 (2009).
[17]A. R. Piriz, L. D. Lucchio, and G. R. Prieto, Phys. Plasmas **18**, 012702 (2011).
[18]H. Qin, R. C. Davidson, and B. G. Logan, Nucl. Instrum. Methods Phys. Res., Sect. A **733**, 203 (2014).
[19]S. Kawata, Phys. Plasmas **19**, 024503 (2012).
[20]K. Nishikawa, J. Phys. Soc. Jpn. **24**, 916 (1968).
[21]G. J. Morales, Y. C. Lee, and R. B. White, Phys. Rev. Lett. **32**, 457 (1974).
[22]D. R. Nicholson, Phys. Fluids **24**, 908 (1981).
[23]C. S. Liu and V. K. Tripathi, *Interaction of Electromagnetic Waves with Electron Beams and Plasmas* (World Scientific, Singapore, 1994), pp. 125–128.
[24]V. K. Tripathi and C. S. Liu, Phys. Fluids **25**, 629 (1982).
[25]V. K. Tripathi, S. T. Tsai, and C. S. Liu, Phys. Fluids **27**, 170 (1984).
[26]N. Ahmad, V. K. Tripathi, M. Rafat, and M. M. Husain, Phys. Plasmas **16**, 062308 (2009).
[27]S. P. Kuo, Phys. Plasmas **9**, 1456 (2002).